Kinetics of Cellulose Conversion at 25 MPa in Sub- and Supercritical Water

Mitsuru Sasaki
Genesis Research Institute, Inc., 4-1-35 Noritake-shinmachi, Nishi-ku, Nagoya 451-0051, Japan

Tadafumi Adschiri
Institute of Multidisciplinary Research for Advanced Materials, Tohoku University, 2-1-1 Katahira, Aoba-ku, Sendai 980-8577, Japan

Kunio Arai
Dept. of Chemical Engineering, Faculty of Engineering, Tohoku University, 7 Aza-Aoba, Aramaki, Aoba-ku, Sendai 980-8579, Japan

Experiments of microcrystalline cellulose conversion in subcritical and supercritical water were conducted at temperatures between 290 and 400°C, a pressure of 25 MPa, and residence times of 0.02–13.1 s using a continuous-flow-type microreactor. First, the reaction mechanism of microcrystalline cellulose in subcritical and supercritical water was proposed on the basis of detailed product analyses. Next, the kinetic description of this reaction in subcritical and supercritical water using a grain model was carried out to verify the proposed reaction mechanism and consequently found that the reaction-rate models were able to express the reaction of microcrystalline cellulose at identical conditions. © 2004 American Institute of Chemical Engineers *AIChE J,* 50: 192–202, 2004
Keywords: microcrystalline cellulose; supercritical water; subcritical water; reaction kinetics

Introduction

Cellulose is the most abundant biological polysaccharide that all plants and algae have. This is contained in municipal solid wastes and agricultural resources, namely biomass resource. Development of an effective utilization process of biomass and cellulose has been expected as one of the postpetrochemical methods that can solve a food problem caused by the rapid increase in the population worldwide and the energy problem from a lack of fossil fuels (Danner and Braun, 1999; Goldstein, 1975).

Cellulose is a β-(1, 4) linked homopolymer of many anhydroglucose residues and can be easily hydrolyzed using acid catalysts (Farone and Cuzens, 1997; Kim et al., 2001; Lee et al., 2001) and enzymes (Mandels et al., 1974; Bhat and Bhat, 1997; Ortega et al., 2001) to cellooligosaccharides and glucose, which are biologically precious chemical intermediates for organic synthesis and fermentation, and so forth. Also, cellulose derivitization such as esterification and etherification has been conventionally performed in aqueous alkali hydroxide solutions, special organic solvents, and metal-complex solvents (Klemm et al., 1998). The reason why these solvents and enzymes have been used for the hydrolysis and derivation of cellulose is because of the presence of intra- and intermolecular hydrogen bond linkages at the crystalline region in cellulose. The presence of intramolecular hydrogen bonds is responsible for chain stiffness and stability of the conformation, and the presence of intermolecular hydrogen bonds makes water solubility and reactivity of the functional groups to solvents de-

Correspondence concerning this article should be addressed to M. Sasaki at this current address: Dept. of Applied Chemistry and Biochemistry, Faculty of Engineering, Kumamoto University, 2-39-1 Kurokami, Kumamoto 860-8555, Japan.

crease. As a result, development of any effective and environmentally benign recycling process of cellulose seems to have been impossible, as long as it can swell or dissolve only in those solvents.

Water at around the critical point (T_c = 374.2°C, P_c = 22.1 MPa, and ρ_c = 0.323 g · cm^{-3}) shows some unique properties (Akiya and Savage, 2002), and has been considered as a reaction medium for various organic reactions (Savage, 1999; Bröll et al., 1999; Ikushima et al., 2000; Taylor et al., 2001; Katritzky et al., 2001; Sato et al., 2001; Akiya and Savage, 2001; Ito et al., 2001; Sasaki et al., 2003). Research regarding the conversion of cellulose and cellulosic biomass to valuable chemical intermediates using water at hydrothermal and supercritical conditions have been reported (Saka and Ueno, 1999; Schmieder et al., 2000; Antal et al., 2000; Ehara and Saka, 2002; Sakaki et al., 2002). Also in our laboratory, the reaction kinetics of cellulose and its related saccharides in subcritical and supercritical water has been studied for the purpose of understanding their reaction features at identical conditions. Recently, the major reaction paths of cellulose in subcritical and supercritical water were found to be hydrolysis, retro-aldol condensation, keto-enol tautomerism, and dehydration (Kabyemela et al., 1997a, b, c, 1998, 1999; Goto et al., 2001; Ehara et al., 2002). It was also found that these reaction rates could be controlled by manipulating the temperature and pressure in near- and supercritical water without catalysts (Kabyemela et al., 1998; Goto et al., 2001; Sasaki et al., 1998, 2000, 2002a, b; Adschiri et al., 1993). Especially, the experimental finding that cellulose was able to swell or dissolve in high-temperature and high-pressure water was obtained through the *in situ* observation of its phase behavior using a diamond anvil cell (Sasaki et al., 2000). These results permit us to develop a new green conversion method that can produce valuable chemical intermediates from cellulose and its related biomass with near- and supercritical water. However, before now a detailed reaction mechanism under these conditions has not been clarified.

In this study, we first conducted experiments of the microcrystalline cellulose conversion in subcritical and supercritical water by using a continuous-flow-type microreactor and then measured its conversion rates at identical conditions. Next, based on the results of the kinetic analysis and the detailed analyses of the products and residues recovered from the experiments, we tried to propose the reaction mechanism for microcrystalline cellulose. Further, we developed a reaction-rate model that was able to describe the reactions of microcrystalline cellulose in subcritical and supercritical water.

Experimental and Analytical Methods

Experimental methods

Microcrystalline cellulose from Merck (Avicel No. 2331—mean particle size: 20–100 μm; a viscosity average degree of polymerization (DP_V): 230; a relative crystallinity (χ_c): 77.8%) was used in this study. Experiments of the microcrystalline cellulose conversion were carried out in temperature ranges of 320–400°C, a pressure of 25 MPa, and residence times of 0.02–13.1 s using the continuous-flow-type microreactor shown in Figure 1. At first, distilled water was fed into a system at a flow rate of 20.0 cm^3 · min^{-1} using three high-performance liquid chromatography (HPLC) pumps (GL Science Ind. Co. Ltd, Model PUS-8), pressurized in the system to a reaction pressure that was controlled at 25 MPa using a back-pressure regulator (TESCOM, Model 26-1721-24), and then preheated up to subcritical or supercritical temperatures using an electric furnace (Seiwa-Riko, Co., Ltd., Model FTO-6). Then the preheated water was mixed with cellulose–water slurries of 10.0 wt. % fed from another line at 5.0 cm^3 · min^{-1} using a slurry feed pump (AKICO Co. Ltd.) at the mixing point in order to rapidly heat up to the reaction temperature, T [°C]. The mixed-slurry solution was then introduced into the reactor tubing. The reaction temperature in the reactor was measured by a K-type thermocouple (1/16-in. OD) at a distance of about 20 mm from the mixing tee. The reactor was covered with heat insulation when the reactor length was short, so the temperature hardly decreased. In the case where the reactor length was too short to measure the reaction temperature directly, it was evaluated by the enthalpy balance. From the preliminary experiment, it was found that the variations between the calculated temperatures evaluated by this method and the measured ones were in the range of 1–2°C, while, in the case where the length of the reactor was long, the reactor was immersed in a heated molten salt bath [Parker Michael Ind. Co. Ltd., KNO_3/$NaNO_2$ = 45/55 (w/w)] kept at the reaction temperature to assure constant temperature throughout the reactor. The reactor volume, V [cm^3], was changed from 0.03 cm^3 to 5.27 cm^3 by replacing a reactor of a different length. After passing through the reactor, the reaction solution was quickly quenched to below 60°C to terminate further reaction by using a pump (GL Science Ind. Co. Ltd, Model PUS-8) to inject water into the main stream at 14.0 cm^3 · min^{-1}, and externally by a cooling jacket. It was confirmed that the direct injection of cool water hardly affected the product distribution from the preliminary experiment. The quenched reaction solution was led to the in-line filtration part [each in-line filter (NUPRO, Model SS-4TF-05) has 0.5-μm pore size]. In this part, there are two parallel-line streams. If the system reached a stationary state, the reaction solution was introduced to one side of the filtration part. At this part, the solid portion (e.g., unreacted cellulose and residue) was continuously trapped, while the liquid portion was passed through, depressurized by passing through the back-pressure regulator, and then collected in a sampling bottle for 10–30 min during the experiment. When the desired time had

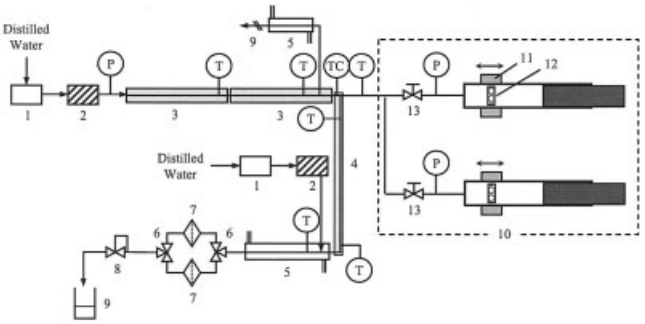

Figure 1. A continuous-flow-type microreactor with a slurry feed pump for cellulose conversion.

1: Degassing unit; 2: high-pressure feed pump; 3: preheating unit; 4: reactor; 5: cooling jacket; 6: three-way valve; 7: in-line filter; 8: back-pressure regulator; 9: sampling bottle; 10: slurry feed pump; 11: permanent magnet; 12: static mixer; 13: needle valve.

passed, sampling of the liquid fraction was finished, and at the same time the collection of the solid fraction was completed by switching the line stream of the reaction solution at the filtration part from the original side to another one. In this study, the experiments were conducted more than three times at each reaction condition. Errors that came from the experiments and analysis were within 5%.

We employed the rapid-heating and quick-quenching method. This method permits us to estimate the accurate V value. The residence time in the reactor, τ (s), was calculated by Eq. 1

$$\tau = \frac{V \cdot \rho}{F \cdot \rho_0} \tag{1}$$

where F ($cm^3 \cdot min^{-1}$) is the flow rate of the slurry solution introduced in the reactor, ρ ($g \cdot cm^{-3}$) is the density of water at the reaction condition, and ρ_0 ($g \cdot cm^{-3}$) is the density of water at the ambient temperature and pressure.

Analytical methods

The liquid product solution was decanted at 20°C for 24 h. In the case where a water-insoluble white precipitate, namely cellulose II, appeared in the solution, it was separated from the water-soluble portion, dried at 60°C for 24 h and then weighed, W_{II} (g). The Cellulose II yield, Y_{II}, was calculated by Eq. 2

$$Y_{II} = \frac{W_{II}}{W_0} \tag{2}$$

The composition of a water-soluble product solution was analyzed by HPLC (Thermoquest Co. Ltd., Model Spectra System AS3000) with a refraction index (RI) detector (ERC, Model 7515A). Details of the HPLC analysis are given in a previous work (Sasaki et al., 2000). Product yield of component i, Y_i, was calculated as a carbon basis by Eq. 3

$$Y_i = \frac{W_i}{W_0} \cdot \frac{a_{C,0}}{b_{C,i}} \tag{3}$$

where $a_{c,0}$ is the carbon number of an anhydroglucose unit in cellulose and $b_{c,i}$ is the carbon number of component i. The Y_S is the yield of water-soluble saccharides (cellohexaose, cellopentaose, cellotetraose, cellotriose, cellobiose and glucose), and the Y_D is the yield of aqueous degradation products of glucose [erythrose, glycolaldehyde, fructose, glyceraldehyde, dihydroxyacetone, pyruvaldehyde, 1,6-anhydro-β-D-glucose and 5-hydroxymethyl-2-furaldehyde (5-HMF)].

The solid portion recovered at the filtration part during the experiment was dried at 60°C for 24 h and subsequently weighed, W_R (g). Conversion of cellulose, X, was calculated by Eq. 4 from the weight change of cellulose before and after the experiment:

$$X = 1 - \frac{W_R}{W_0} \tag{4}$$

Measurement of macromolecular characteristics of the cellulose II and residue

Macromolecular properties of the water-insoluble cellulose II, which was obtained from the liquid product solution, and the residue, which was recovered at the filtration part, were investigated by the following analyses.

FT-IR Analysis. FT-IR spectra of the cellulose II and residue were recorded by a diffusional reflection method on a FT-IR spectrometer (Biorad, Japan) under the following operating conditions: resolution, 2 cm^{-1}; accumulation, 32; interpolation, 0; window function, triangle.

X-Ray Diffraction Analysis. X-Ray diffraction (XRD) patterns of the cellulose II and residue were recorded by an X-ray diffraction analyzer (MAC Science Co. Ltd., Model M18XHF22-SRA) in the 2θ range of 5° to 20°, using a Mo-K_α radiation (wavelength: 0.71423 nm). Relative crystallinity indexes of the cellulose II and residue, χ_c, were calculated by the following equation with Segal's method (Segal et al., 1945)

$$\chi_c = \frac{I_{(200)} - I_{am}}{I_{(200)}} \tag{5}$$

The content of the amorphous region in each solid portion, χ_{am}, was calculated as

$$\chi_{am} = 1 - \chi_c \tag{6}$$

where $I_{(200)}$ and I_{am} are peak intensities corresponding to (200) plane ($2\theta = 9.98°$) and amorphous ($2\theta = 8.40°$) for cellulose I. For cellulose II, $I_{(200)}$ and I_{am} are $2\theta = 9.00°$ and 6.00°, respectively.

Viscosity-Average Degree of Polymerization (DP_V). The DP_V of the solid portion was determined as follows (Lindsay, 1981). A solid sample weighing 0.5 g (dry basis) was added to a 1.5 cm^3 cadoxen solution (cadmium oxide/ethyenediamine/$NaOH/H_2O$ = 5/28/166/14 (w/w/w/w) at 25°C and maintained at less than 10°C for 24 h with stirring, to swell and dissolve into the cadoxen solution. Then, a viscosity-average molecular weight of the solid sample, M_V, was evaluated by determining the limiting viscosity number [η] using the Mark-Houwink-Sakurada equation shown in Eq. 7. The DP_V was obtained by Eq. 8

$$[\eta] = 1.84 \cdot M_V^{0.76} \tag{7}$$

$$DP_V = \frac{M_V}{162} \tag{8}$$

Results and Discussion

Product distribution

Liquid Products. Figure 2a–2c show the yields of the main products at 320°, 350°, and 400°C at 25 MPa. The main products of the microcrystalline cellulose conversion were hydrolysis products (water-insoluble cellulose II and water-soluble saccharides), aqueous degradation products of glucose (fructose, erythrose, glycolaldehyde, glyceraldehyde, 5-HMF, etc.), and undetected aqueous products that were probably organic acids (e.g., acetic acid and formic acid). No char and

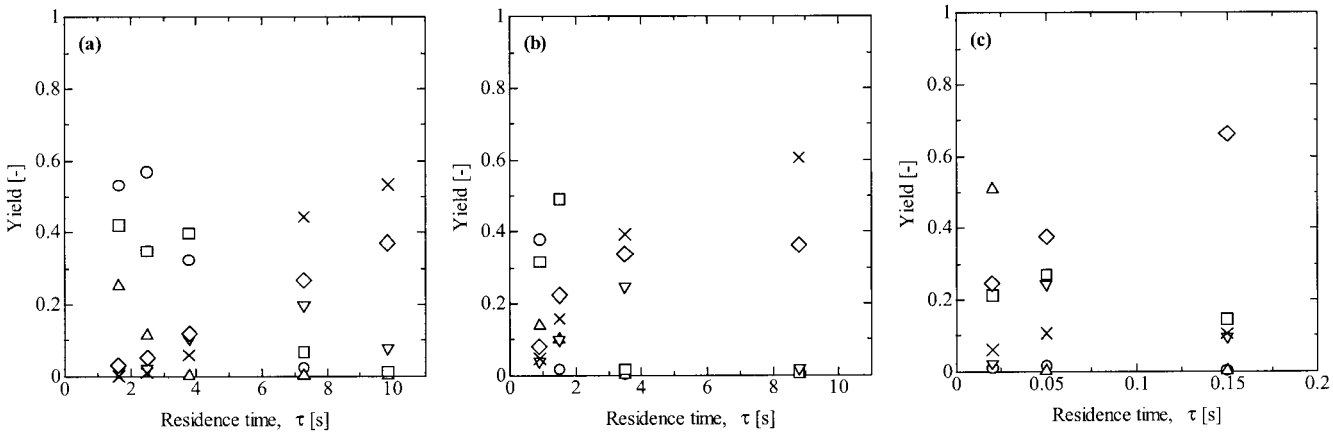

Figure 2. The yields of cellulose II and water-soluble saccharides on the reaction of microcrystalline cellulose in subcritical and supercritical water at 25 MPa.

(a) 320°C; (b) 375°C; (c) 400°C. Symbols: ○, residue; △, cellulose II; □, water-soluble cellooligosaccharides; ▽, glucose; ◇, aqueous degradation products of glucose; ×, acids.

tar were formed in all the reaction conditions. At 320°C, the yields Y_{II} and Y_S increased with time and reached, respectively, 28% and 40% at 1.8 s. By increasing the residence time, their yields decreased, while the Y_D increased due to further hydrolysis of the cellulose II and saccharides formed. The yield of undetected aqueous products also became higher when the residence time was increased. At 350°C, the variation of the main products was similar to that at 320°C. In contrast, in supercritical water at 400°C, microcrystalline cellulose rapidly converted to water-insoluble cellulose II and water-soluble saccharides, and yields Y_{II} and Y_S reached about 50% and 30% at 0.02 s, respectively, while yield Y_D scarcely increased even for extended residence times.

The DP_V of the water-insoluble cellulose II obtained from the liquid product solution was determined. Figure 3 shows the relationship between the DP_V of the cellulose II and X at 25 MPa. The DP_V values ranged from 40 to 50 and slightly decreased to about 35 at higher conversions, and it seems that this trend does not depend upon the reaction temperature in the range between 320 and 385°C at 25 MPa. At 400°C, nearly half of microcrystalline cellulose converted to the cellulose II with a DP_V of about 40 at almost a 100% conversion level.

Solid Residue. Figure 4 shows the relationship between the average DP_V of the residue and X at various temperatures and 25 MPa. In all cases except 400°C, it seems that the DP_V of the residue monotonically decreased from 230 (an initial DP_V) to about 50 as the reaction progressed. This indicates that the cellulose conversion follows the same reaction mechanism at the subcritical and supercritical conditions we employed.

The variation of the χ_c of the residue as a function of X is shown in Figure 5. The χ_c of the residue has almost the same values as that of untreated microcrystalline cellulose (78.3%). This result shows that the cellulose conversion occurs hetero-

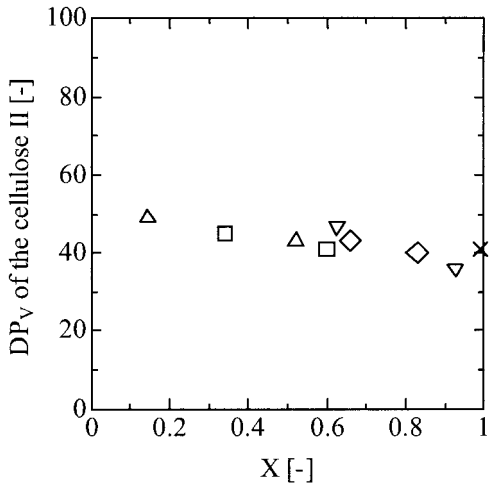

Figure 3. The plot of the viscosity average degree of polymerization (DP_V) of the water-insoluble cellulose II as it appears in the aqueous product solution vs. the conversion of cellulose (X).

Symbols: ○, 320°C; △, 355°C; □, 370°C; ▽, 375°C; ◇, 385°C; ×, 400°C.

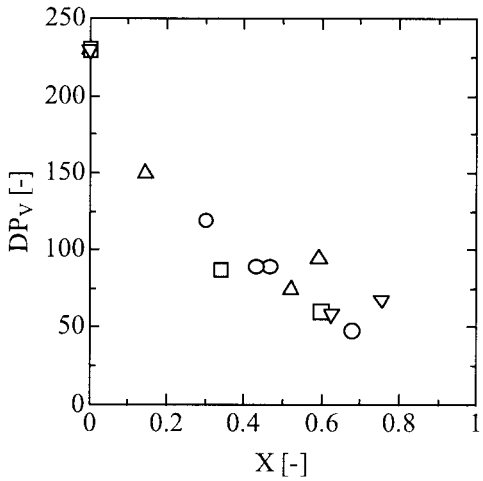

Figure 4. Viscosity average degree of polymerization (DP_V) of residues as a function of the X at 25 MPa.

Symbols: ○, 320°C; △, 355°C; □, 370°C; ▽, 375°C.

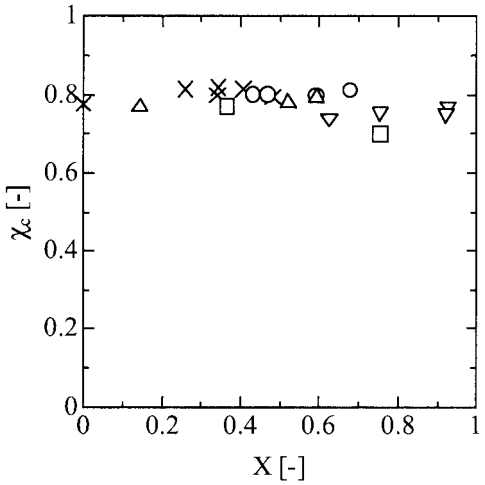

Figure 5. Relative crystallinity index of the residue (χ_c) as a function of the X at 25 MPa.

Symbols: ×, 290°C; ○, 320°C; △, 355°C; □, 370°C; ▽, 375°C.

geneously by maintaining its crystal structure at 290–380°C and 25 MPa. In addition, the crystal polymorphs of the residues were investigated by XRD. Figure 6a and 6b show the variations of the XRD patterns of the residues as a function of X at 320 and 375°C, respectively. At 320°C, all the residues had only the cellulose I crystal form at high conversion levels, while at 375°C two diffraction peaks corresponding to the cellulose II crystal form appeared in the XRD patterns of the residues, even at low conversions. Also, the diffraction intensities of the cellulose II crystal form increased with the reaction. In general, most of celluloses have only the cellulose I crystal form. The cellulose II crystal form exists in mercerized celluloses and regenerated celluloses, which must have been conventionally produced through the mercerization (dissolution) of the native celluloses using aqueous alkaline solutions. Therefore, it can be seen that swelling or dissolution of microcrystalline cellulose occurs during the reaction in near- and supercritical water.

Overall conversion rate of microcrystalline cellulose

In our previous work, it was found that hydrolysis of cellulose particles mainly took place at their external or inner (pore) surface in subcritical water (Sasaki et al., 1998, 2000). Also, Yoshioka et al. (1998, 2001) reported that the rate of hydrolysis of poly(ethylene terephthalate) (PET) particles followed a shrinking-core model under hydrothermal conditions. From these experimental findings, it seems that this surface reaction-rate model is applicable to describe the microcrystalline cellulose conversion in subcritical and supercritical water, and thus it was employed

$$\frac{dV(X)}{dt} = -k_S \cdot S(X) \tag{9}$$

where k_S (cm · s^{-1}) is the surface reaction-rate constant, and S (cm^2) and V (cm^3) are the surface area and the volume of the particle, respectively. Here, from the well-known knowledge that a cellulose particle consisted of a large number of microfibrils, and that the microfibril comprises a number of crystallites that are combined in series, it is supposed that a cylindrical-shaped grain is more suitable than the sphere-shaped grain for microcrystalline cellulose. Therefore, the model with cylindrical grain was employed. In this model, a solid particle is assumed to be composed of cylindrical grains of radius r_g (μm). Since the conversion of cellulose, X, is $X = 1 - (V(X)/V(0)) = 1 - (W(X)/W(0))$, the conversion rate can be expressed as

$$\frac{dX}{dt} = 2 \cdot \frac{k_S}{r_{g,0}} (1 - X)^{1/2} \tag{10}$$

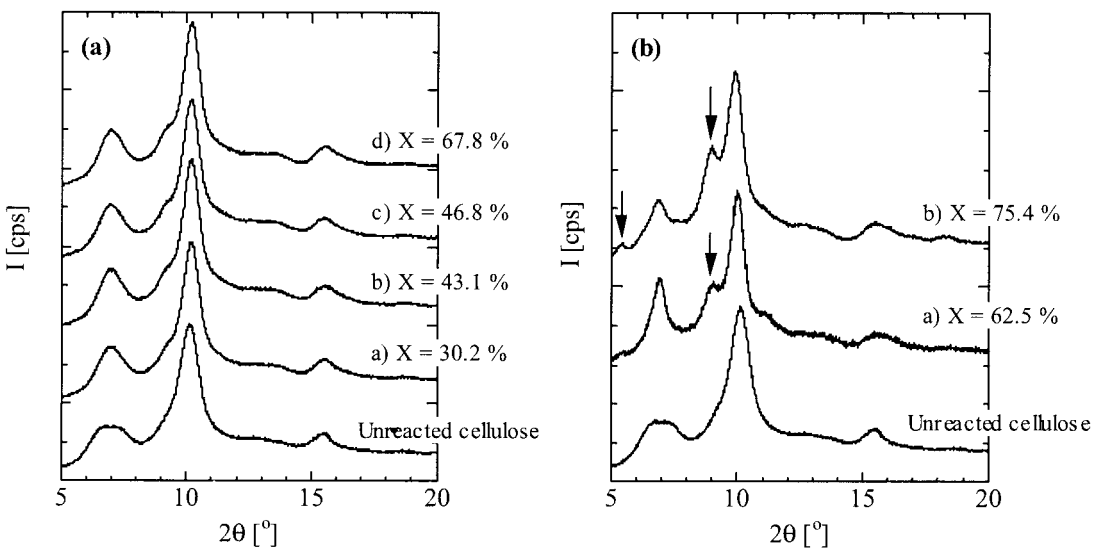

Figure 6. Variation of the XRD patterns of the residues on the conversion of microcrystalline cellulose in subcritical and supercritical water at 25 MPa.

(a) 320°C and (b) 375°C. Arrows stand for the diffraction peaks of cellulose II crystal.

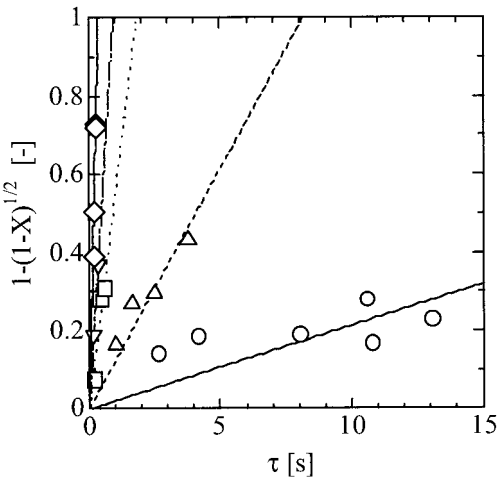

Figure 7. Relationship between the $1 - (1 - X)^{1/3}$ and the residence time (τ) on the reaction of microcrystalline cellulose in subcritical and supercritical water at 25 MPa.

Symbols: ×, 290°C; ○, 320°C; △, 355°C; □, 370°C; ▽, 375°C.

where $r_{g,0}$ (μm) is the initial radius of each grain.

By integrating this equation, the following equation was obtained

$$k = \frac{k_S}{r_{g,0}} = \frac{1 - (1 - X)^{1/2}}{\tau} \tag{11}$$

where k (s^{-1}) is the overall conversion rate constant of microcrystalline cellulose.

The $1 - (1 - X)^{1/2}$ values at all the reaction conditions were plotted against the residence time, τ (s). Figure 7 shows typical results at 320, 375, and 400°C and 25 MPa. The $1 - (1 - X)^{1/2}$ values were proportional to τ in all the temperatures, indicating that the microcrystalline cellulose conversion can be described by this reaction-rate model under the subcritical and supercritical conditions. At each reaction condition, the k value was determined from the slope of the straight line in this figure. Figure 8 shows the Arrhenius plot of the k values obtained in the range of 320–400°C at 25 MPa. The x-axis represents a reciprocal temperature, $1000/T$ (K^{-1}), and the y-axis indicates a logarithm of the k value, $\ln(k\ (s^{-1}))$. From this figure, it was found that the microcrystalline cellulose conversion in subcritical and supercritical water consisted of two Arrhenius-type reactions with a crosspoint of about 370°C. Below 370°C, the reaction was heterogeneous surface hydrolysis of cellulose without its swelling microcrystalline cellulose, and the apparent activation energy, E_a, and the preexponential factor, A, of this region were 145.9 ± 4.6 kJ mol^{-1} and $10^{11.9\pm0.4}$, respectively. In contrast, above 370°C the conversion rate of microcrystalline cellulose became much faster than that below 370°C, and the kinetic parameters were found to be $E_a = 547.9 \pm 27.8$ kJ · mol^{-1} and $A = 10^{44.6\pm2.2}$, respectively. The main reasons for this drastic change in the conversion rate of microcrystalline cellulose are due to the contributions of (1) swelling or dissolution, and (2) pyrolytic depolymerization of microcrystalline cellulose. The former is supported by the analytical finding that all the residues recovered from the experiments below 350°C had both the cellulose II crystal form and the cellulose I crystal form. Also, as regards the latter, Bühler et al. (2002) pointed out the possibility that the reaction mechanism shifted from an ionic reaction mechanism to a radical one by decreasing the water density by increasing the temperature at constant pressure in supercritical water. This knowledge suggests that the contribution of pyrolytic depolymerization as well as that of swelling or dissolution of microcrystalline cellulose to its overall conversion rate may increase at higher temperatures at constant pressure in supercritical water. This matter will be clarified in the near future.

Reaction mechanism

As was described in the section titled "Product distribution," the crystal structure of the residue had only the cellulose I crystal form at 320°C, even at higher conversions, while the residues recovered from the experiments at higher temperatures had both the cellulose I and II crystal forms, even at low conversions, and also the intensities of the diffraction peaks corresponding to the cellulose II crystal form became higher with the reaction. From these experimental and analytical findings, it can be seen that understanding the relationship between the cellulose II crystal content in the residue and the conversion of cellulose may lead to the elucidation of the reaction mechanism of microcrystalline cellulose in subcritical and supercritical water.

Here, the cellulose II crystal content in the residue (θ_{II}) was determined in the following. First, the intensities of three diffraction peaks corresponding to (200), (110), and (1–10) planes of the cellulose I crystal were recorded ($I_{I(200)}$, $I_{I(110)}$, $I_{I(1-10)}$, respectively) from the XRD pattern of untreated microcrystalline cellulose. The relative intensity ratios of the pure cellulose I crystal, $I_{I(110)}/I_{I(200)}$ and $I_{I(1-10)}/I_{I(200)}$, were calculated as 0.1046 and 0.3663, respectively. In the same way, the XRD pattern of a filtration paper, which has the cellulose II crystal form, was recorded and the relative intensity ratios of

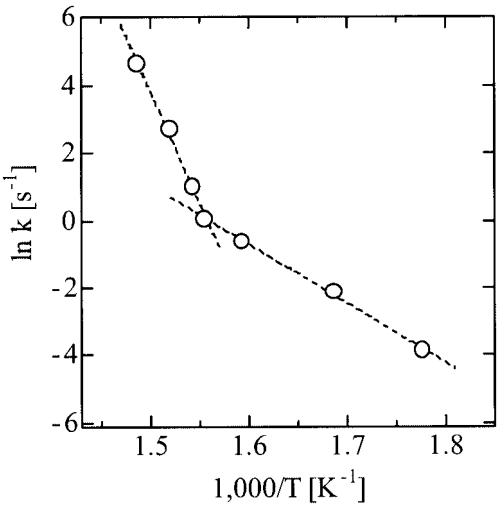

Figure 8. Arrhenius plot of the rate constant of conversion of microcrystalline cellulose (k) in subcritical and supercritical water at 25 MPa based on the shrinking-core (or grain) model.

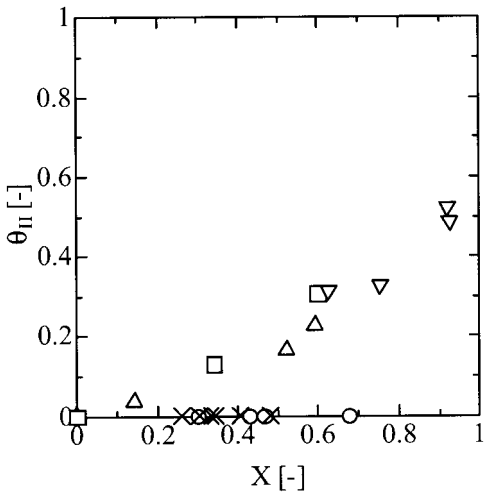

Figure 9. The content of the cellulose II crystal form in the residue (θ_{II}) as a function of the *X* at 25 MPa.

Symbols: ×, 290°C; ○, 320°C; △, 355°C; □, 370°C; ▽, 375°C.

the pure cellulose II crystal, $I_{II(110)}/I_{II(200)}$ and $I_{II(1-10)}/I_{II(200)}$, were calculated as 0.3703 and 1.1752, respectively. In this case, both the absolute intensities of the (200) plane of the untreated microcrystalline cellulose and the filtration paper were almost the same, so it was assumed that the II(200) was the same as the I(200). Next, assuming that each relative intensity ratio of the (110) and (1–10) planes to the (200) plane was shown in the linear function of the conversion of cellulose, then the cellulose II crystal contents at these planes in the residue, $\theta_{II(110)}$ and $\theta_{II(1-10)}$, were calculated by the following equations

$$\theta_{II(110)} = \left(\frac{I_{II}}{I_I}\right)_{(110)} = 3.4381 \cdot \left(\frac{I_{II(110)}}{I_{II(200)}}\right) - 0.3643 \qquad (12)$$

$$\theta_{II(1-10)} = \left(\frac{I_{II}}{I_I}\right)_{(1-10)} = 1.2424 \cdot \left(\frac{I_{II(1-10)}}{I_{I(200)}}\right) - 0.4601 \qquad (13)$$

The θ_{II} of the residue was consequently calculated by averaging the two values using Eq. 14

$$\theta_{II} = \frac{1}{2}\left(\theta_{II(110)} + \theta_{II(1-10)}\right) \qquad (14)$$

Figure 9 shows the plot of the θ_{II} values as a function of *X* at 25 MPa. The cellulose II crystal content in the residue was 0 in all the conversions at low temperatures (e.g., 290 and 320°C). In contrast, the θ_{II} values increased with the reaction at 355–385°C, but the trend scarcely depended upon the reaction temperature. These results indicate that the conversion of microcrystalline cellulose occurs at around the crystal surface without swelling or dissolution in subcritical water (290–320°C), while swelling or dissolution of microcrystalline cellulose occurs during the reaction at the near- and supercritical conditions. In this case, it can be expected that concentrated regions that consist of amorphous-like cellulose molecules form at around the crystal surface of microcrystalline cellulose, and thus the reactivity of the concentrated regions in microcrystalline cellulose increases. As a result, the conversion rate of microcrystalline cellulose can be promoted in near- and supercritical water.

In this study, the following two experimental findings were also determined:

(1) The relative crystallinity (χ_c) of the residues kept nearly the same high values as that of untreated microcrystalline cellulose.

(2) The variation in the DP_V of all the residues showed the same trend against the conversion of cellulose (X).

The reason for the former is as follows. Microcrystalline cellulose is the high crystalline cellulose that is removed from any amorphous region by alkaline pretreatments, so we can assume that the main reaction is hydrolysis in the surface region of microcrystalline cellulose. In near- and supercritical water, the cellulose can swell or dissolve at around the surface region to form the amorphous-like region. But it is easily hydrolyzed to water-soluble saccharides during the reaction or recrystallized as the cellulose II crystal region on the residue after the reaction. Consequently, the relative crystallinity of the residue hardly changes irrespective of the reaction temperature, although the amount of residue may become small with the reaction.

Following is another explanation for the latter. It is well known that cellulose consists of a large number of microfibrils and each microfibril comprises a number of crystallites. Because the amorphous region in microcrystalline cellulose is negligibly small, it is supposed that the main reaction is hydrolysis at the surface region of the particle, microfibrils, or crystallites. The fact that the DP_V of the residues monotonically decreased from 230 to about 50 with the reaction, regardless of the reaction temperature, shows that hydrolysis of microcrystalline cellulose does not take place at the surface of the cellulose particle. If hydrolysis occurs only at the particle surface of microcrystalline cellulose, almost no decrease in the DP_V of the residues will be observed at low conversions. Additionally, the DP_V profile shown in Figure 4 should not be displayed if the main reaction is either swelling of a microfibril and the subsequent cleavage of the microfibril to crystallites (Figure 10a), or cleavage of a microfibril to crystallites and the subsequent swelling of the crystallites (Figure 10b). Accordingly, the main reaction in near-critical and supercritical water can be supposed to be the combination of these two reactions.

When all the experimental and analytical findings are considered, the reaction mechanism of microcrystalline cellulose in subcritical and supercritical water can be proposed as shown in Figure 11. When a crystallite is taken up, cellulose molecules in the crystallite line in parallel and form intermolecular hydrogen bond networks among the molecules. In subcritical water, the crystallite is hydrolyzed at the surface region without swelling or dissolving as shown in the upper part of this figure. Therefore, the overall conversion rate of microcrystalline cellulose is slow and no cellulose II crystal can be formed in the residue. In contrast, in near- and supercritical water, the crystallite can swell or dissolve around the surface region to form amorphous-like cellulose molecules. These molecules are inactive, so they can be easily hydrolyzed to lower *DP* celluloses

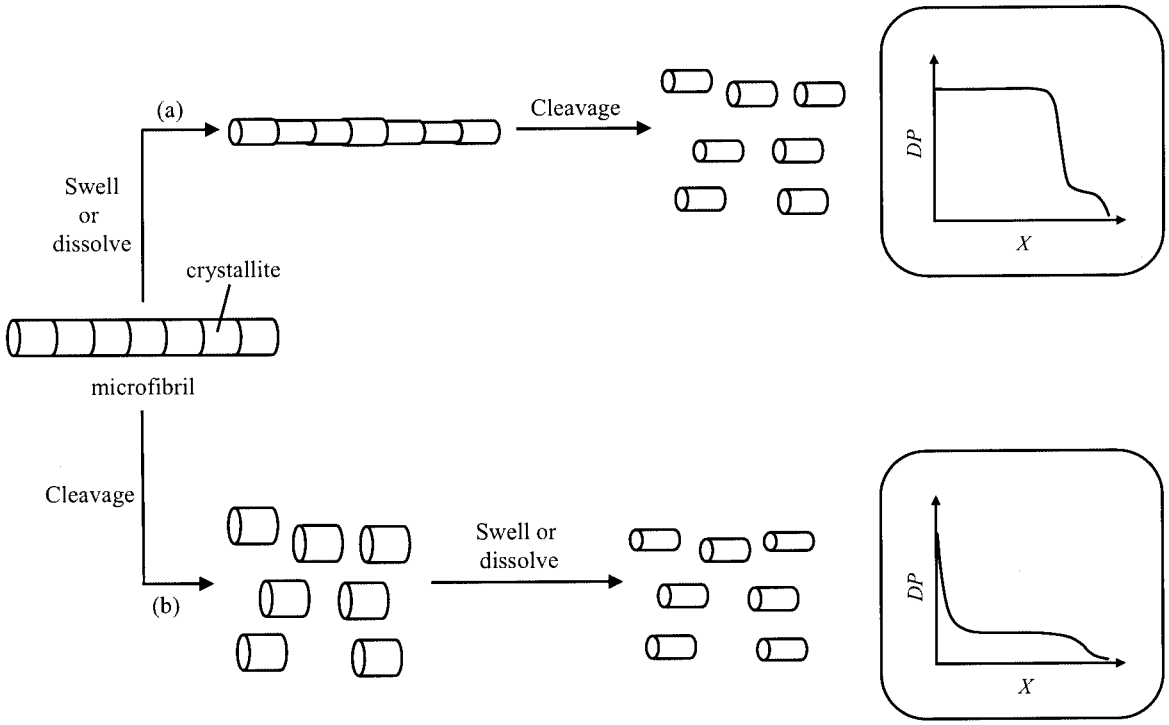

Figure 10. The typical variations of the *DP* of the residues.

(a) In the case where the main reaction is the swelling of a microfibril and subsequent cleavage of the microfibril to crystallites; and (b) in the case where the main reaction is cleavage of the microfibril to crystallites and subsequent swelling of the crystallites.

and cellooligosaccharides. Some of the hydrolysates can pass from the polymer phase to water phase by cleavage of their hydrogen bond networks, while others remain on the crystallite surface of the residue. The liberated portion in the water phase is further hydrolyzed to water-soluble saccharides, or crystallized as water-insoluble cellulose II after the reaction. On the other hand, the amorphous-like portion remaining in the polymer phase is hydrolyzed to water-soluble saccharides, or swells further or dissolves and moves from the polymer phase to the water phase. As a consequence, the overall conversion rate of microcrystalline cellulose can become faster than that in near- and subcritical water. Also, relatively high *DP* cellulose II and water-soluble saccharides can be obtained from high yields under identical conditions.

Reaction-rate models for the microcrystalline cellulose conversion in near- and supercritical water

To verify the proposed reaction mechanism of microcrystalline cellulose in near- and supercritical water, we tried to describe the experimental results by the grain model by swelling or dissolution of the cellulose crystallite. In this model, a cylindrical grain with an initial internal radius of $r_{g,0}$ shrinks to the grain of radius r_g via its surface hydrolysis. It is thought that the outer surface of the crystallite swells or dissolves in near- and supercritical water, which is recrystallized as the cellulose II crystal in the residue after the reaction and decantation. As a result, the residue comprises the inner cellulose I crystal region (internal radius: r_g) and the outer cellulose II crystal region (thickness: r_{II}). Here, a relationship between the radii of the cylindrical grain and X can be expressed by

$$\frac{r_g + r_{II}}{r_{g,0}} = (1 - X)^{1/2} \tag{15}$$

Assuming that the thickness of the outer cellulose II crystal region, r_{II}, is very small compared with that of the inner cellulose I crystal region, r_I, in the grain, Eq. 15 can be rewritten as

$$r_g = r_{g,0} \cdot (1 - X)^{1/2} \tag{16}$$

It also can be supposed that the volumetric ratio of the cellulose II crystal region to the cellulose I crystal region in the residue is proportional to the value θ_{II} estimated from the XRD analysis. The θ_{II} value can be expressed as follows

$$\theta_{II} = \frac{I_{II} \cdot w_{II}}{I_I \cdot w_I} = \frac{I_{II,0} \cdot (2\pi r_g \cdot r_{II} \cdot l \cdot \rho_{II})}{I_{I,0} \cdot (\pi r_g^2 \cdot l \cdot \rho_I)} = 2 \cdot \frac{I_{II,0} \cdot \rho_{II}}{I_{I,0} \cdot \rho_I} \cdot \frac{r_{II}}{r_g} \tag{17}$$

Diffraction intensities of the cellulose I and II crystal forms ($I_{I,0}$ and $I_{II,0}$) corresponding to each (200) plane are almost the same sensitivity, and the bulk density of the cellulose I crystal is almost identical to that of the cellulose II crystal (1.6 g cm^{-3}). Therefore, Eq. 17 can be simplified to Eq. 18

$$\theta_{II} \approx 2 \cdot \frac{r_{II}}{r_g} \tag{18}$$

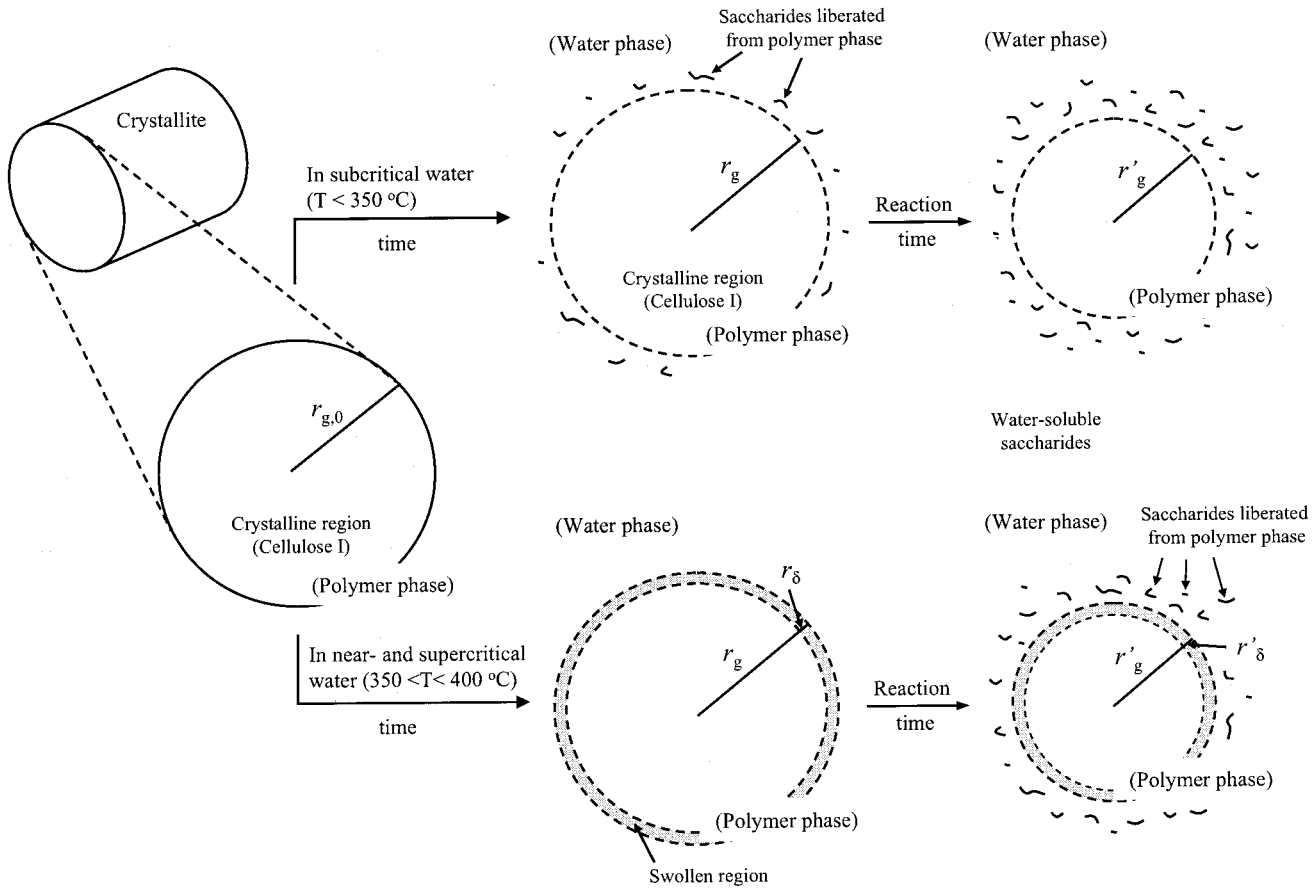

Figure 11. Estimated reaction mechanism for the conversion of microcrystalline cellulose in subcritical and supercritical water.

We introduce Eq. 16 into Eq. 18 to obtain Eq. 19. This equation can be also rewritten as Eq. 20

$$\theta_{II} = 2 \cdot \frac{r_{II}}{r_{g,0}} (1 - X)^{-1/2} \tag{19}$$

$$\ln(\theta_{II}) = ln\left(2 \cdot \frac{r_{II}}{r_{g,0}}\right) - \frac{1}{2} \cdot \ln(1 - X) \tag{20}$$

If the reaction model is suitable for describing the experimental results, a slope of the straight line obtained ideally must be 0.5. We carried out the least-square fitting of the experimental data and found that the data at near-critical temperatures (350–375°C) and 25 MPa could be expressed as a straight line whose slope was 0.527 ± 0.110, as shown in Figure 12. This indicates that the main reaction of microcrystalline cellulose in near-critical water is heterogeneous hydrolysis with the crystallite surface region swelling or dissolving.

On the other hand, we could not recover any solid residue on the experiments at 400°C, because the conversion rate of microcrystalline cellulose was very fast. Thus, we could not carry out the preceding kinetic analysis. At the supercritical temperature of 400°C, it was found that nearly half the microcrystalline cellulose was converted to the relatively high *DP* (30–50) cellulose II. Here, it was assumed that microcrystalline cellulose rapidly swelled and dissolved into supercritical water to form the homogeneous phase and then hydrolyzed to lower *DP* celluloses and water-soluble saccharides. In general, a

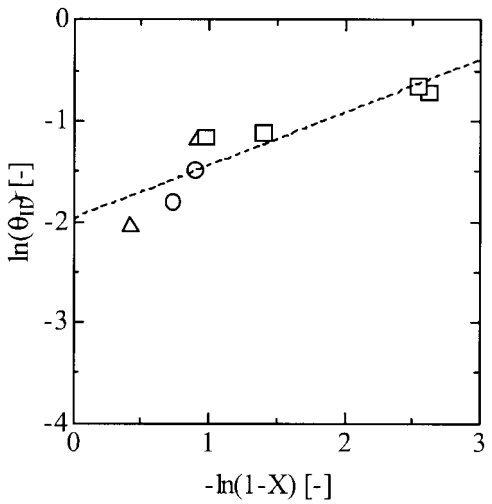

Figure 12. Relationship between $\ln(\theta_{II})$ and $-\ln(1 - X)$ in near-critical water at 25 MPa.

Symbols: ○, 350–355°C; △, 370°C; □, 375°C.

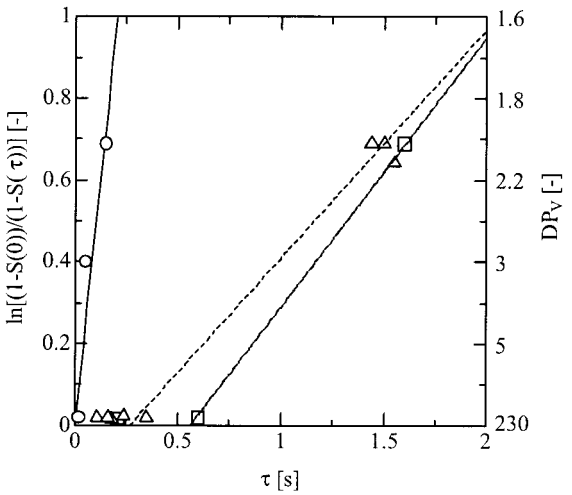

Figure 13. Kinetic analysis on hydrolysis of microcrystalline cellulose in subcritical and supercritical water at 25 MPa by using a homogeneous first-order rate law.

Symbols: ○, 400°C; △, 370–385°C; □, 350–355°C.

homogeneous hydrolysis rate can be expressed using the first-order rate law (Matthes, 1942; Sato et al., 1998) as described below

$$\frac{dS}{dt} = k' \cdot (1 - S) \tag{21}$$

$$\ln\left(\frac{1 - S(0)}{1 - S(\tau)}\right) = k' \cdot \tau \tag{22}$$

where $S(0)$ and $S(\tau)$ are degrees of splitting at $t = 0$ and τ, respectively [$S(0) = 1/DP(0)$, $S(\tau) = 1/DP(\tau)$], and k' is the first-order hydrolysis rate constant [s^{-1}].

In the case of the microcrystalline cellulose conversion, the $\ln[(1 - S(0))/(1 - S(\tau))]$ values calculated from the average molecular-weight distributions at each residence time at 400°C were plotted against the residence time. Figure 13 shows the result. Data at subcritical (350–355°C) and near-critical (370–385°C) temperatures are also plotted in this figure. At 400°C, the data were consistent with the proportional line, while the data at subcritical and near-critical temperatures disagreed with the straight lines which pass through. From this result, it is suggested that hydrolysis of microcrystalline cellulose at 400°C takes place homogeneously.

Conclusions

In this study, we investigated the reaction kinetics and mechanism on the microcrystalline cellulose conversion in subcritical and supercritical water through detailed experiments and analyses of the products and residues at a pressure of 25 MPa. As a result, we successfully proposed the reaction mechanism for microcrystalline cellulose in subcritical and supercritical water, and also established that the increase in the conversion rate of microcrystalline cellulose at near- and supercritical conditions was caused by the acceleration of the conversion by the swelling or dissolution of the crystalline cellulose under the same conditions. Moreover, we developed the reaction-rate models for this reaction in near-critical and supercritical water, thereby verifying that these models were able to describe the experimental and analytical results with relatively high accuracy. Future efforts will be directed toward investigating the effect of the reaction pressure (or the density of water) on reactions of microcrystalline cellulose in subcritical and supercritical water.

Acknowledgment

The authors gratefully acknowledge support by a Grand-in-Aid for Scientific Research on Priority Area "Mechanism of Hydrolysis in Supercritical Water" (#11450295) from the Ministry of Education, Culture, Sports, Science and Technology.

Literature Cited

Adschiri, T., S. Hirose, R. M. Malaluan, and K. Arai, "Noncatalytic Conversion of Cellulose in Supercritical and Subcritical Water," *J. Chem. Eng. Jpn.,* **26**(6), 676 (1993).

Akiya, N., and P. E. Savage, "Kinetics and Mechanism of Cyclohexanol Dehydration in High-Temperature Water," *Ind. Eng. Chem. Res.,* **40**(8), 1822 (2001).

Akiya, N., and P. E. Savage, "Roles of Water for Chemical Reactions in High-Temperature Water," *Chem. Rev.,* **102**(8), 2725 (2002).

Antal, M. J., Jr., S. G. Allen, D. Schulman, X. Xu, and R. J. Divilio, "Biomass Gasification in Supercritical Water," *Ind. Eng. Chem. Res.,* **39**(11), 4040 (2000).

Bhat, M. K., and S. Bhat, "Cellulose Degrading Enzymes and Their Potential Industrial Applications," *Biotechnol. Adv.,* **15,** 583 (1997).

Bröll, D., C. Kaul, A. Krämer, P. Krammer, T. Richter, M. Jung, H. Vogel, and P. Zehner, "Chemistry in Supercritical Water," *Angew. Chem. Int. Ed.,* **38,** 2998 (1999).

Bühler, W., E. Dinjus, H. J. Ederer, A. Kruse, and C. Mas, "Ionic Reactions and Pyrolysis of Glycerol as Competing Reaction Pathways in Near- and Supercritical Water," *J. Supercr. Fluids,* **22,** 37 (2002).

Danner, H., and R. Braun, "Biotechnology for the Production of Commodity Chemicals from Biomass," *Chem. Soc. Rev.,* **28,** 395 (1999).

Ehara, K., and S. Saka, "A Comparative Study on Chemical Conversion of Cellulose Between the Batch-Type and Flow-Type Systems in Supercritical Water," *Cellulose,* **9,** 301 (2002).

Farone, W., and J. E. Cuzens, "Method of Producing Sugars Using Strong Acid Hydrolysis of Cellulosic and Hemicellulosic Materials," *Biotechnol. Adv.,* **15**(2), 538 (1997a).

Goldstein, I. S., "Potential for Converting Wood into Plastics," *Science,* **189,** 847 (1975).

Goto, K., K. Tajima, M. Sasaki, T. Adschiri, and K. Arai, "Reaction Mechanism of Sugar Derivatives in Subcritical and Supercritical Water," *Kobunshi Ronbunshu,* **58**(12), 685 (2001).

Ikushima, Y., K. Hatakeda, O. Sato, T. Yokoyama, and M. Arai, "Acceleration of Synthetic Organic Reactions Using Supercritical Water: Noncatalytic Beckmann and Pinacol Rearrangements," *J. Amer. Chem. Soc.,* **122**(9), 1908 (2000).

Ito, H., J. Nishiyama, T. Adschiri, and K. Arai, "Synthesis of ϵ-Caprolactam from ϵ-Caprolactone and Ammonia in Supercritical Water," *Kobunshi Ronbunshu,* **58**(12), 679 (2001).

Kabyemela, B. M., T. Adschiri, R. M. Malaluan, and K. Arai, "Kinetics of Glucose Epimerization and Decomposition in Subcritical and Supercritical Water," *Ind. Eng. Chem. Res.,* **36**(5), 1552 (1997a).

Kabyemela, B. M., T. Adschiri, R. M. Malaluan, and K. Arai, "Degradation Kinetics of Dihydroxyacetone and Glyceraldehyde in Subcritical and Supercritical Water," *Ind. Eng. Chem. Res.,* **36,** 2025 (1997b).

Kabyemela, B. M., T. Adschiri, R. M. Malaluan, K. Arai, and H. Ohzeki, "Rapid and Selective Conversion of Glucose to Erythrose in Supercritical Water," *Ind. Eng. Chem. Res.,* **36**(12), 5063 (1997c).

Kabyemela, B. M., M. Takigawa, T. Adschiri, and K. Arai, "Mechanism and Kinetics of Cellobiose Decomposition in Sub- and Supercritical Water," *Ind. Eng. Chem. Res.,* **37**(2), 357 (1998).

Kabyemela, B. M., T. Adschiri, R. M. Malaluan, and K. Arai, "Glucose and Fructose Decomposition in Subcritical and Supercritical Water: Detailed

Reaction Pathway, Mechanisms, and Kinetics," *Ind. Eng. Chem. Res.,* **38**(8), 2888 (1999).
Katritzky, A. R., D. A. Nichols, M. Siskin, R. Murugan, and M. Balasubramanian, "Reactions in High-Temperature Aqueous Media," *Chem. Rev.,* **101**(4), 837 (2001).
Kim, J. S., Y. Y. Lee, and R. W. Torget, "Cellulose Hydrolysis Under Extremely Low Sulfuric Acid and High-Temperature Conditions," *Appl. Biochem. Biotechnol.,* **92**(1–3), 331 (2001).
Klemm, D., B. Philipp, T. Heinze, U. Heinze, and W. Wagenknecht, *Comprehensive Cellulose Chemistry,* Vol. 2, *Functionalization of Cellulose,* WILEY-VCH, Weinheim (1998).
Lindsay, W. T., "Hydrogen Bonding and Water Structure," *ASME Handbook on Water Technology for Thermal Power Systems,* P. Cohen, ed., ASME, New York (1981).
Mandels, M., L. Hontz, and J. Nystrom, "Enzymatic Hydrolysis of Waste Cellulose," *Biotechnol. Bioeng.,* **26,** 1471 (1974).
Matthes, A., *Kolloid-Z.,* **98,** 319–339 (1942).
Ortega, N., M. D. Busto, and M. Perez-Mateos, "Kinetics of Cellulose Saccharification by *Trichoderma reesei* Cellulases," *Int. Biodeterior. Biodegrad.,* **47**(1), 7 (2001).
Saka, S., and T. Ueno, "Chemical Conversion of Various Celluloses to Glucose and Its Derivatives in Supercritical Water," *Cellulose,* **6,** 177 (1999).
Sakaki, T., M. Shibata, T. Sumi, and S. Yasuda, "Saccharification of Cellulose Using a Hot-Compressed Water-Flow Reactor," *Ind. Eng. Chem. Res.,* **41,** 661 (2002).
Sasaki, M., B. M. Kabyemela, R. M. Malaluan, S. Hirose, N. Takeda, T. Adschiri, and K. Arai, "Cellulose Hydrolysis in Subcritical and Supercritical Water," *J. Supercrit. Fluids,* **13,** 261 (1998).
Sasaki, M., Z. Fang, Y. Fukushima, T. Adschiri, and K. Arai, "Dissolution and Hydrolysis of Cellulose in Sub- and Supercritical Water," *Ind. Eng. Chem. Res.,* **39**(8), 2883 (2000).
Sasaki, M., K. Goto, K. Tajima, T. Adschiri, and K. Arai, "Rapid and Selective Retro-Aldol Condensation of Glucose to Glycolaldehyde in Supercritical Water," *Green Chem.,* **4**(3), 285 (2002a).
Sasaki, M., M. Furukawa, K. Minami, T. Adschiri, and K. Arai, "Kinetics and Mechanism of Cellobiose Hydrolysis and Retro-Aldol Condensation in Subcritical and Supercritical Water," *Ind. Eng. Chem. Res.,* **41,** 6642 (2002b).
Sasaki, M., J. Nishiyama, M. Uchida, K. Goto, K. Tajima, T. Adschiri, and K. Arai, "Conversion of Hydroxyl Group in 1-Hexyl Alcohol to Amide Group in Supercritical Water Without Catalyst," *Green Chem.,* **5**(1), 95 (2003).
Sato, H., K. Kondo, S. Tsuge, H. Ohtani, and N. Sato, "Mechanisms of Thermal Degradation of a Polyester Flame-Retarded with Antimony Oxide/Brominated Polycarbonate Studied by Temperature-Programmed Analytical Pyrolysis," *Polym. Degradation Stab.,* **62,** 41 (1998).
Sato, T., G. Sekiguchi, T. Adschiri, and K. Arai, "Non-Catalytic and Selective Alkylation of Phenol with Propane-2-ol in Supercritical Water," *Chem. Commun.,* 1566 (2001).
Savage, P. E., "Organic Chemical Reactions in Supercritical Water," *Chem. Rev.,* **99**(2), 603 (1999).
Schmieder, H., J. Abeln, N. Boukis, E. Dinjus, A. Kruse, M. Kluth, G. Petrich, E. Sadri, and M. Schacht, "Hydrothermal Gasification of Biomass and Organic Wastes," *J. Supercrit. Fluids,* **17,** 145 (2000).
Segal, L., J. J. Creely, A. E. Martin, Jr., and C. M. Conrad, "An Empirical Method for Estimating the Degree of Crystallinity of Native Cellulose Using the X-Ray Diffractometer," *Textile Res. J.,* **29**(10), 786 (1959).
Taylor, J. D., J. I. Steinfeld, and J. W. Tester, "Experimental Measurement of the Rate of Methyl *tert*-Butyl Ether Hydrolysis in Sub- and Supercritical Water," *Ind. Eng. Chem. Res.,* **40**(1), 67 (2001).
Yoshioka, T., N. Okayama, and A. Okuwaki, "Kinetics of Hydrolysis of PET Powder in Nitric Acid by a Modified Shrinking-Core Model," *Ind. Eng. Chem. Res.,* **37,** 336 (1998).
Yoshioka, T., T. Motoki, and A. Okuwaki, "Kinetics of Hydrolysis of Poly(ethylene terephthalate) Powder in Sulfuric Acid by a Modified Shrinking-Core Model," *Ind. Eng. Chem. Res.,* **40,** 75 (2001).

Manuscript received Feb. 7, 2003, and revision received May 27, 2003.